

Polarized e-p Elastic Scattering in the Collider Frame

C. Sofiatti

*Department of Physics,
University of Massachusetts Boston,
100 Morrissey Blvd., Boston, MA 02125**

T. W. Donnelly

*Center for Theoretical Physics, Laboratory for Nuclear Science and Department of Physics,
Massachusetts Institute of Technology, Cambridge, MA 02139*

(Dated: April 13, 2011)

Double polarization elastic $\vec{e}\text{-}\vec{p}$ cross sections and asymmetries are considered in collider kinematics. Covariant expressions are derived for the general situation involving crossed beams; these are checked against the well-known results obtained when the proton is at rest. Results are given using modern models for the proton electromagnetic form factors for kinematics of interest in e-p colliders such as the EIC facility which is in its planning stage. In context, parity-violating elastic $\vec{e}\text{-}p$ scattering is compared and contrasted with these double-polarization (parity-conserving) results.

PACS numbers: 12.15.Ji, 13.40.Gp, 13.60.Fz, 25.30.Bf, 29.25.Pj, 29.27.Hj

I. INTRODUCTION

The main focus of this paper is the development of the formalism for polarized $\vec{e}\text{-}\vec{p}$ elastic scattering in the collider frame, stimulated by interest in e-p colliders such as the EIC [1] facility which is in its planning stage. At least two things motivate such a study. (1) One has the possibility of measuring the electromagnetic form factors of the proton in unusual kinematics, that is, with high-energy colliding beams of polarized electrons and protons — to be contrasted to the usual situation with polarized electrons scattering from protons at rest with either the target proton polarized or when the recoiling final-state proton's polarization is measured. Specifically, we shall see that the role played by 2γ corrections to the dominantly one-photon-exchange diagram (the only one we consider in detail in this work) is likely quite different for collider kinematics. (2) One may use the reasonably well-known double-polarization asymmetry to determine the product of the electron and proton polarizations, $p_e p_p$, when the focus is placed on other reactions (*e.g.*, DIS).

The basic kinematical formalism is presented in Sect. II for both collinear and crossed beams. This is followed in Sect. III by developments of the leptonic (electron) and hadronic (proton) tensors needed in discussing parity-conserving double-polarized $\vec{e}\text{-}\vec{p}$ elastic scattering. Here a general frame is considered and all quantities are kept completely covariant so that any situation can be explored, including the special case where the proton is at rest (the “rest frame”) and where the formalism is well known. In Sect. IV the leptonic and hadronic tensors are contracted to yield the invariant matrix element required in constructing the polarized cross sections and asymmetries, while in Sect. V expressions for the latter are presented.

Our approach in this study has been to develop the formalism in detail and thereby to bring out clearly the particular roles played by the different proton form factors. We shall see that the fact that the proton's Pauli form factor is nonzero alters the character of the asymmetry from the simpler answer obtained when colliding point Dirac particles. We retain both the electron and proton masses (*i.e.*, we do not invoke the extreme relativistic limit) so that any choice of kinematics can be explored. In the case of the electron this is not needed except when scattering at very small angles; however, for the proton it is critical to retain the mass terms if one wishes to be able to go to the rest frame. Since the formalism is only a little more involved when keeping all mass terms than to drop them as is often done, we retain them throughout this study.

We shall see that the asymmetries are rather small — the reasons for this will be explained later — and accordingly in Sect. VI we also briefly consider parity-violating elastic $\vec{e}\text{-}p$ scattering in collider kinematics. We shall see that this single-polarization asymmetry is only about one order of magnitude smaller than the double-polarization parity-conserving asymmetries.

In Sect. VII results are presented for two choices of kinematics that may be relevant for a future EIC facility. The asymmetries (PC and PV) are all given, as is the figure-of-merit and thereby the anticipated fractional uncertainty expected given specific collider luminosities and polarizations. The computer code Brasil2011 has been developed to handle any kinematical situation and can be obtained [2] by anyone interested in exploring other conditions that may be relevant when planning for a future e-p collider. Finally, our conclusions are presented in Sect. VIII.

* c.sofiatti@gmail.com

II. BASIC COLLIDER-FRAME KINEMATICS

A. Collinear beams

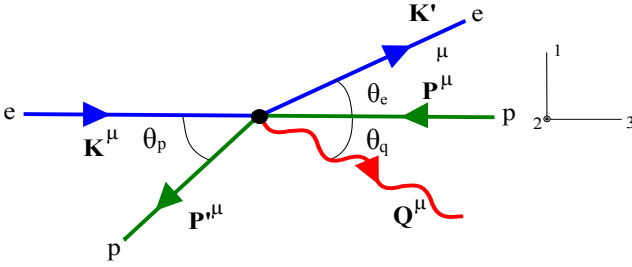


FIG. 1. (color online) Electron-proton elastic scattering in collider kinematics.

The coordinate frame used in this work is shown in Fig. 1; we start with collinear kinematics and then in the following subsection generalize to the situation where the electron and proton beams are crossed. Here an electron with 4-momentum K^μ is incident from the left and a proton with P^μ enters from the right. The final state has an electron with K'^μ scattered at an angle θ_e and a proton with P'^μ scattered at an angle θ_p , as shown. The 4-momentum transfer

$$Q^\mu = K^\mu - K'^\mu = P'^\mu - P^\mu \quad (1)$$

makes an angle θ_q with respect to the beam axis. The 4-momenta in the problem are thus the following: $K^\mu = (\epsilon, \mathbf{k})$, $K'^\mu = (\epsilon', \mathbf{k}')$, $P^\mu = (E, \mathbf{p})$, $P'^\mu = (E', \mathbf{p}')$ and $Q^\mu = (\omega, \mathbf{q})$ with $\mathbf{k} = k\mathbf{u}_3$ and $\mathbf{p} = -p\mathbf{u}_3$. Since the electron and proton are both on-shell, one can write their energies in terms of their 3-momenta: $\epsilon = \sqrt{k^2 + m_e^2}$, $\epsilon' = \sqrt{k'^2 + m_e^2}$, $E = \sqrt{p^2 + m_p^2}$ and $E' = \sqrt{p'^2 + m_p^2}$.

We assume that the variables used to specify the kinematics are (k, p, θ_e) and then through the equations above the energies of the incident particles are also given. It proves useful to define the total 4-momentum

$$P_{tot}^\mu \equiv K^\mu + P^\mu \equiv (E_{tot}, \mathbf{p}_{tot}) \quad (2)$$

$$= K'^\mu + P'^\mu, \quad (3)$$

where Eq. (3) follows by energy-momentum conservation. This implies that

$$E_{tot} = \epsilon + E = \epsilon' + E' \quad (4)$$

$$\mathbf{p}_{tot} = (k - p)\mathbf{u}_3 = p_{tot}\mathbf{u}_3 = \mathbf{k}' + \mathbf{p}'. \quad (5)$$

The square of the total 4-momentum is the invariant

$$s = P_{tot}^2 = E_{tot}^2 - p_{tot}^2 = m_e^2 + m_p^2 + 2\xi, \quad (6)$$

where

$$\xi \equiv \epsilon E + kp \quad (7)$$

is also given by the initial momenta.

Using 3-momentum conservation and given p_{tot} and θ_e , the scattered proton's 3-momentum can be written in terms of the scattered electron's 3-momentum:

$$p' = \sqrt{k'^2 + p_{tot}^2 - 2p_{tot}k' \cos \theta_e} \quad (8)$$

$$\sin \theta_p = \frac{k'}{p'} \sin \theta_e \quad (9)$$

$$\cos \theta_p = \frac{1}{p'} (k' \cos \theta_e - p_{tot}). \quad (10)$$

Additionally, from energy conservation one has that

$$E_{tot}\epsilon' - p_{tot}k' \cos \theta_e = m_e^2 + \xi \quad (11)$$

which constitutes an equation for k' . Solving, one has

$$k' = \frac{1}{a} \left[b + E_{tot} \sqrt{\xi^2 - m_e^2(m_p^2 + p_{tot}^2 \sin^2 \theta_e)} \right] \quad (12)$$

with

$$a \equiv E_{tot}^2 - p_{tot}^2 \cos^2 \theta_e = s + p_{tot}^2 \sin^2 \theta_e \quad (13)$$

$$= m_p^2 + m_e^2 + 2\xi + p_{tot}^2 \sin^2 \theta_e \geq (m_p + m_e)^2 > 0 \quad (14)$$

$$b \equiv (m_e^2 + \xi)p_{tot} \cos \theta_e, \quad (15)$$

and knowing k' one can use the equations given above to determine ϵ' , p' , E' and θ_p . Since the argument of the square root in Eq. (12) must be non-negative one has

$$\xi \geq m_e \sqrt{m_p^2 + p_{tot}^2 \sin^2 \theta_e}. \quad (16)$$

The 4-momentum transfer is also now specified:

$$\omega = \epsilon - \epsilon' \quad (17)$$

$$q = \sqrt{k^2 + k'^2 - 2kk' \cos \theta_e} \quad (18)$$

$$\sin \theta_q = \frac{k'}{q} \sin \theta_e \quad (19)$$

$$\cos \theta_q = \frac{1}{q} (k - k' \cos \theta_e). \quad (20)$$

From Eqs. (17) and (18), together with the energy-momentum relationships above one has

$$Q^2 = t = -2(\epsilon\epsilon' - kk' \cos \theta_e - m_e^2) \quad (21)$$

$$= - \left[4kk' \sin^2 \theta_e / 2 + \frac{2m_e^2(k - k')^2}{\epsilon\epsilon' + kk' + m_e^2} \right] \leq 0, \quad (22)$$

that is, the 4-momentum transfer is spacelike [3].

To conclude this brief discussion of the basic collinear kinematics, it is instructive to express the kinematic variables above in the proton rest frame. For any 4-vector in the collider frame the corresponding quantities in the proton rest frame may be found by boosting in the \mathbf{u}_3 direction by $\beta_p \equiv p/E$ with $\gamma_p = E/m_p = [1 - \beta_p^2]^{-1/2}$. In particular, the proton in its rest frame of course has

$P^\mu = (m_p, 0, 0, 0)$ while the incident electron has 3-momentum and energy given by

$$k_{rest} = \gamma_p(k + \beta_p \epsilon) \quad (23)$$

$$\epsilon_{rest} = \gamma_p(\epsilon + \beta_p k). \quad (24)$$

For the scattered electron one has

$$\epsilon'_{rest} = \gamma_p(\epsilon' + \beta_p k' \cos \theta_e) \quad (25)$$

$$k'_{rest} = \sqrt{(\epsilon'_{rest})^2 - m_e^2} \quad (26)$$

$$\sin \theta_e^{rest} = \frac{k' \sin \theta_e}{k'_{rest}} \quad (27)$$

$$\cos \theta_e^{rest} = \frac{\gamma_p(k' \cos \theta_e + \beta_p \epsilon')}{k'_{rest}}. \quad (28)$$

To get some feeling for the extreme nature of the kinematics typically of interest (see Sect. VII), we consider two choices for the kinematics, I. $k = 10$ GeV/c with $p = 250$ GeV/c and II. $k = 2$ GeV/c with $p = 50$ GeV/c (see also Table I in Sect. VII). For the former high-energy case we have $\beta_p \approx 1$, $\gamma_p \approx 250$, so $k_{rest} \approx 500k = 5$ TeV/c and $\sin \theta_e^{rest} \approx \sin \theta_e / 500$. This means that for this choice of kinematics and, for instance, for 1° (5°) scattering in the collider frame the equivalent rest frame (for example, for fixed target measurements) has an incident electron beam of 5.3 TeV/c scattering at 0.002° (0.01°). For the lower-energy case II. we have again for 1° (5°) scattering in the collider frame that the equivalent rest frame has an incident electron beam of 213 GeV/c with scattering angle 0.009° (0.047°).

Any of the other kinematic variables above may be related to their rest-frame equivalents in a similar manner.

B. Crossed beams

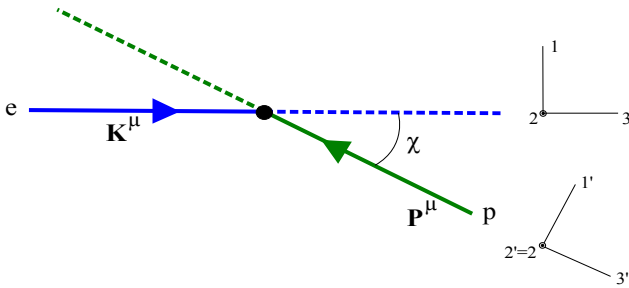


FIG. 2. (color online) Electron-proton elastic scattering in crossed-beams collider kinematics.

In this subsection we provide the extensions that are necessary when the electron and proton beams are not collinear, but are crossed. The kinematics for this are shown in Fig. 2. The electron is assumed to be incident along the \mathbf{u}_3 -axis as before; however, now the proton beam is assumed to have its momentum \mathbf{p} directed along

the $-\mathbf{u}_{3'}$ -axis where the $(1', 2', 3')$ system is rotated from the $(1, 2, 3)$ through an angle χ as shown. Clearly

$$\mathbf{u}_1 = \cos \chi \mathbf{u}_{1'} - \sin \chi \mathbf{u}_{3'} \quad (29)$$

$$\mathbf{u}_3 = \sin \chi \mathbf{u}_{1'} + \cos \chi \mathbf{u}_{3'}. \quad (30)$$

Let us repeat the kinematics developments of the previous subsection, now working in the $(1', 2', 3')$ system where we have $\mathbf{k} = k(\sin \chi \mathbf{u}_{1'} + \cos \chi \mathbf{u}_{3'})$ and $\mathbf{p} = -p \mathbf{u}_{3'}$. E_{tot} in Eq. (4) is as before; however, now we have

$$\mathbf{p}_{tot} = k \sin \chi \mathbf{u}_{1'} + (k \cos \chi - p) \mathbf{u}_{3'}, \quad (31)$$

yielding

$$p_{tot}^2 = k^2 + p^2 - 2kp \cos \chi \quad (32)$$

and therefore

$$s = P_{tot}^2 = E_{tot}^2 - p_{tot}^2 = m_e^2 + m_p^2 + 2\hat{\xi}, \quad (33)$$

where

$$\hat{\xi} = \epsilon E + kp \cos \chi; \quad (34)$$

cf. Eq. (7). The extension of Eq. (8) is

$$p' = \sqrt{k'^2 + p_{tot}^2 - 2k'(k \cos \theta_e - p \cos(\theta_e + \chi))} \quad (35)$$

and of Eqs. (9,10) are

$$\sin(\theta_p + \chi) = \frac{1}{p'} [k' \sin(\theta_e + \chi) - k \sin \chi] \quad (36)$$

$$\cos(\theta_p + \chi) = \frac{1}{p'} [k' \cos(\theta_e + \chi) - (k \cos \chi - p)], \quad (37)$$

from which the angle θ_p may be found by taking the inverse sine and cosine. The analog of Eq. (11) is

$$E_{tot} \epsilon' - k' p_{cross}^{\parallel} = m_e^2 + \hat{\xi}, \quad (38)$$

where for convenience we have defined

$$p_{cross}^{\parallel} \equiv k \cos \theta_e - p \cos(\theta_e + \chi) \quad (39)$$

$$p_{cross}^{\perp} \equiv k \sin \theta_e - p \sin(\theta_e + \chi). \quad (40)$$

One then has that

$$k' = \frac{1}{\hat{a}} \left[\hat{b} + E_{tot} \sqrt{\hat{\xi}^2 - m_e^2(m_p^2 + [p_{cross}^{\perp}]^2)} \right] \quad (41)$$

with

$$\hat{a} \equiv E_{tot}^2 - [p_{cross}^{\parallel}]^2 = s + [p_{cross}^{\perp}]^2 \quad (42)$$

$$= m_p^2 + m_e^2 + 2\hat{\xi} + [p_{cross}^{\perp}]^2 \quad (43)$$

$$\hat{b} \equiv (m_e^2 + \hat{\xi}) p_{cross}^{\parallel}. \quad (44)$$

The rest of the developments go through as before in the collinear case.

III. LEPTONIC AND HADRONIC TENSORS

For the leptonic (here electron) tensor one has

$$\eta_{\mu\nu} = \frac{1}{2} [\eta_{\mu\nu}^{unpol} + \eta_{\mu\nu}^{pol}], \quad (45)$$

where, following standard developments [4], the unpolarized tensor (symmetric under $\mu \leftrightarrow \nu$) is given by

$$2m_e^2 \eta_{\mu\nu}^{unpol} = \frac{1}{2} Q^2 \left(g_{\mu\nu} - \frac{Q_\mu Q_\nu}{Q^2} \right) + 2R_\mu R_\nu \quad (46)$$

with

$$R_\mu \equiv \frac{1}{2} (K_\mu + K'_\mu). \quad (47)$$

The polarized tensor (antisymmetric under $\mu \leftrightarrow \nu$) is given by

$$2m_e^2 \eta_{\mu\nu}^{pol} = i \epsilon_{\mu\nu\alpha\beta} (m_e S_e^\alpha) Q^\beta, \quad (48)$$

where it can be shown [4] that the general spin 4-vector is given by

$$m_e S_e^\alpha = h_e \epsilon \left(\beta_e \cos \mu_e, \cos \mu_e \mathbf{u}_L^e + \frac{1}{\gamma_e} \sin \mu_e \mathbf{u}_\perp^e \right). \quad (49)$$

Here \mathbf{u}_L^e is a unit vector pointing along \mathbf{k} and \mathbf{u}_\perp^e is transverse to this direction. As usual, one has $\beta_e = k/\epsilon$ and $\gamma_e = \epsilon/m_e = [1 - \beta_e^2]^{-1/2}$. Also, the factor $h_e = \pm 1$ is introduced simply to make it easy to switch the electron's polarization from along the beam direction to opposite to it. From this equation one sees that transverse polarizations are suppressed by the relativistic γ -factor and so henceforth we consider only longitudinally polarized incident electrons:

$$m_e S_{e,L}^\alpha = h_e \epsilon (\beta_e, \mathbf{u}_L^e). \quad (50)$$

This yields only three distinct cases for the polarized electron tensor. Since the tensor is antisymmetric under $\mu \leftrightarrow \nu$ we can restrict our attention to cases where $\mu < \nu$, the others being given by using the antisymmetry. The nonzero cases are then:

$$2m_e^2 \eta_{\mu\nu}^{pol} = -i h_e z_{\mu\nu}, \quad (51)$$

where

$$z_{\mu\nu} \equiv \begin{cases} K \cdot Q = \epsilon\omega - kq \cos \theta_q = \frac{1}{2} Q^2 & \mu\nu = 12 \\ \epsilon q \sin \theta_q = \epsilon k' \sin \theta_e & \mu\nu = 02 \\ kq \sin \theta_q = k k' \sin \theta_e & \mu\nu = 23 \end{cases} \quad (52)$$

One can verify that $Q^\mu z_{\mu\nu} = 0$, as should be the case.

Again restricting our attention to collinear beams at first, the proton's polarization 4-vector is similar to the one for the electron in Eq. (49), namely

$$m_p S_p^\alpha = h_p E \left(\beta_p \cos \mu_p, \cos \mu_p \mathbf{u}_L^p + \frac{1}{\gamma_p} \sin \mu_p \mathbf{u}_\perp^p \right). \quad (53)$$

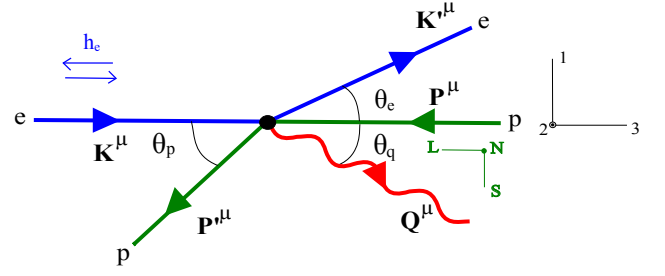


FIG. 3. (color online) The electron polarization is assumed to be along the 3-axis while the proton may be polarized longitudinally (L: along the negative 3-axis) or sideways (S: along the negative 1-axis), as shown.

In the case of the proton we must remember that it is moving to the left and thus, with L for longitudinal, S for sideways and N for normal, one has

$$\mathbf{u}_L^p = -\mathbf{u}_3 \quad (54)$$

$$\mathbf{u}_\perp^p = \cos \eta_p \mathbf{u}_S^p + \sin \eta_p \mathbf{u}_N^p, \quad (55)$$

where $\mathbf{u}_S^p = -\mathbf{u}_1$ and $\mathbf{u}_N^p = \mathbf{u}_2$; see Fig. 3. We shall specify the proton polarization by choosing it to be along the L, S and N directions and then any general case (for instance, when treating crossed beams; see below) can be decomposed into components along these three orthogonal directions. It is worthwhile to reiterate that the conventions used here have +L polarization when it points in the $-\mathbf{u}_3$ direction, +S polarization when it points in the $-\mathbf{u}_1$ direction and +N polarization when it points in the $+\mathbf{u}_2$ direction. One finds that

$$[S_p^\alpha]_L = h_p \gamma_p (\beta_p, -\mathbf{u}_3) \quad (56)$$

$$[S_p^\alpha]_S = h_p (0, -\mathbf{u}_1) \quad (57)$$

$$[S_p^\alpha]_N = h_p (0, -\mathbf{u}_2). \quad (58)$$

Now, for the hadronic (here proton) tensor one has the analogs of the leptonic tensors:

$$W^{\mu\nu} = \frac{1}{2} [W_{unpol}^{\mu\nu} + W_{pol}^{\mu\nu}], \quad (59)$$

where the symmetric unpolarized tensor is given by

$$W_{unpol}^{\mu\nu} = -W_1 \left(g^{\mu\nu} - \frac{Q^\mu Q^\nu}{Q^2} \right) + \frac{1}{m_p^2} W_2 T^\mu T^\nu \quad (60)$$

with

$$T^\mu \equiv \frac{1}{2} (P'^\mu + P^\mu). \quad (61)$$

The invariant functions $W_{1,2}$ (functions only of Q^2) are given as usual in terms of the proton's electromagnetic Sachs form factors by

$$W_1 = \tau (G_M^p)^2 \quad (62)$$

$$W_2 = \frac{1}{1 + \tau} [(G_E^p)^2 + \tau (G_M^p)^2], \quad (63)$$

where $\tau \equiv |Q^2|/4m_p^2 \geq 0$. The antisymmetric polarized proton tensor is given by

$$W_{pol}^{\mu\nu} = -\frac{i}{m_p} G_M^p \left[G_M^p \epsilon^{\mu\nu\alpha'\beta'} S_{\alpha'}^p Q_{\beta'} \right. \\ \left. + \frac{F_2^p}{m_p^2} \left(\epsilon^{\mu\alpha'\beta'\gamma'} T^\nu - T^\mu \epsilon^{\nu\alpha'\beta'\gamma'} \right) S_{\alpha'}^p T_{\beta'} Q_{\gamma'} \right] \quad (64)$$

$$\equiv -ih_p \gamma_p \frac{1}{m_p} G_M^p Z^{\mu\nu} \quad (65)$$

with

$$Z^{\mu\nu} \equiv G_M^p Z_1^{\mu\nu} + \frac{1}{m_p^2} F_2^p Z_2^{\mu\nu} \quad (66)$$

$$Z_1^{\mu\nu} \equiv \frac{h_p}{\gamma_p} \epsilon^{\mu\nu\alpha'\beta'} S_{\alpha'}^p Q_{\beta'} \quad (67)$$

$$Z_2^{\mu\nu} \equiv \frac{h_p}{\gamma_p} \left(\epsilon^{\mu\alpha'\beta'\gamma'} T^\nu - T^\mu \epsilon^{\nu\alpha'\beta'\gamma'} \right) S_{\alpha'}^p T_{\beta'} Q_{\gamma'}. \quad (68)$$

One can verify that $Q_\mu Z^{\mu\nu} = 0$ as should be the case; in fact, $Q_\mu Z_1^{\mu\nu} = Q_\mu Z_2^{\mu\nu} = 0$. For reasons that will become clear in the following section, in these expressions it proves useful to use a mixture of the Sachs magnetic form factor with the Pauli form factor; the Sachs and Dirac/Pauli form factors are related in the familiar way:

$$G_E^p = F_1^p - \tau F_2^p \quad G_M^p = F_1^p + F_2^p \quad (69) \\ F_1^p = \frac{1}{1+\tau} [G_E^p + \tau G_M^p] \quad F_2^p = \frac{1}{1+\tau} [G_M^p - G_E^p]$$

IV. CONTRACTIONS OF LEPTONIC AND HADRONIC TENSORS

We start by obtaining the contraction of the two symmetric unpolarized tensors, namely

$$X^{unpol} \equiv \{2m_e^2 \eta_{\mu\nu}^{unpol}\} \times \{W_{unpol}^{\mu\nu}\} \quad (70)$$

$$= -W_1 \left(\frac{3}{2} Q^2 + 2R^2 \right) \quad (71) \\ + \frac{1}{m_p^2} W_2 \left(\frac{1}{2} Q^2 T^2 + 2(R \cdot T)^2 \right).$$

One has $\frac{3}{2} Q^2 + 2R^2 = Q^2 + 2m_e^2$ and $T^2 = m_p^2 - Q^2/4$ and, using the fact that

$$R \cdot T = K \cdot P + Q^2/4 = \xi + Q^2/4, \quad (72)$$

one therefore has

$$\frac{1}{2} Q^2 T^2 + 2(R \cdot T)^2 = 2 \left[\xi^2 + \frac{1}{2} Q^2 \xi + \frac{1}{4} m_p^2 Q^2 \right]. \quad (73)$$

Defining dimensionless variables $\lambda \equiv \omega/2m_p$ and $\kappa \equiv q/2m_p$, where then $\tau = \kappa^2 - \lambda^2$, as usual, and defining

$$\tilde{\epsilon} \equiv \xi/m_p^2, \quad (74)$$

one then has

$$X^{unpol} \equiv -W_1 (Q^2 + 2m_e^2) \\ + 2m_p^2 W_2 [\tilde{\epsilon}^2 - 2\tau\tilde{\epsilon} - \tau] \quad (75)$$

To connect with standard notation let us use the following [5]

$$V_0 \equiv 4m_p^2 [\tilde{\epsilon}^2 - 2\tau\tilde{\epsilon} - \tau] \quad (76)$$

$$= 4m_p^2 \left[\left(\frac{1}{2m_p^2} \{(\epsilon + \epsilon')E + (k + k' \cos \theta_e)p\} \right)^2 \right. \\ \left. - \tau(1 + \tau) \right] \quad (77)$$

$$\tan^2 \theta'_e/2 \equiv \frac{-Q^2}{V_0} = \frac{\tau}{\tilde{\epsilon}^2 - 2\tau\tilde{\epsilon} - \tau} \quad (78)$$

and then

$$X^{unpol} = \frac{2m_p^2 \tau}{\tan^2 \theta'_e/2} F^2(\tau, \theta_e) \quad (79)$$

where, defining

$$\mathcal{E}' \equiv \left[1 + 2(1 + \tau) \tan^2 \theta'_e/2 \left(1 + \frac{2m_e^2}{Q^2} \right) \right]^{-1}, \quad (80)$$

one has for the total (squared) e-p scattering form factor

$$F^2(\tau, \theta_e) = W_2 + 2W_1 \tan^2 \theta'_e/2 \left(1 + \frac{2m_e^2}{Q^2} \right) \quad (81)$$

$$= \frac{1}{(1 + \tau) \mathcal{E}'} \left[\mathcal{E}' (G_E^p)^2 + \tau (G_M^p)^2 \right]. \quad (82)$$

It is useful at this point to check this general result for the special case of the laboratory frame; there $p = 0$ and so $E = m_p$; also $\lambda_{lab} = \tau$ and $\kappa_{lab} = \sqrt{\tau(1 + \tau)}$. This implies that $\xi_{lab} = m_p \epsilon$ and thus $\tilde{\epsilon}_{lab} = \epsilon/m_p$ and then in the lab. system one can show that $V_0^{lab} = v_0 = (\epsilon + \epsilon')^2 - q^2$, the usual answer [4], and one then has

$$X_{lab}^{unpol} \equiv \frac{1}{2} v_0 F^2(\tau, \theta_e). \quad (83)$$

Furthermore, in the electron Extreme Relativistic Limit (ERL_e) where the electron's mass may be neglected with respect to its momentum, $\theta'_e \rightarrow \theta_e$, $\mathcal{E}' \rightarrow \mathcal{E}$ (the usual so-called virtual photon longitudinal polarization) and the expression above becomes proportional to $\mathcal{E} (G_E^p)^2 + \tau (G_M^p)^2$, the familiar answer.

For the contraction of the two antisymmetric tensors we have from the expressions above

$$X^{pol} \equiv \{2m_e^2 \eta_{\mu\nu}^{pol}\} \times \{W_{pol}^{\mu\nu}\} \quad (84)$$

$$= -h_e h_p \gamma_p \frac{1}{m_p} G_M^p z_{\mu\nu} Z^{\mu\nu}, \quad (85)$$

where $Z^{\mu\nu}$ may be decomposed into $Z_1^{\mu\nu}$ and $Z_2^{\mu\nu}$ as in Eq. (66). Since the choice of longitudinal electron polarization led to only the components $\mu\nu = 12, 02$ and 23

(together with their reverses, which, using the antisymmetry, leads to an overall factor of 2 if only this order is retained), we have only three cases to consider. Furthermore, note that all cases here have either μ or ν equal to 2 and so the proton polarization cannot have component 2. Since this is the only component for N polarization (see Eq. (58)) we find that the proton's polarization (in one-photon-exchange approximation) *cannot be normal*, as expected. For the tensors of type 1 the results are the following:

$$[Z_1^{\mu\nu}]_L = \begin{cases} \omega + \beta_p q \cos \theta_q = -Q^2/2E & \mu\nu = 12 \\ -q \sin \theta_q & \mu\nu = 02 \\ -\beta_p q \sin \theta_q & \mu\nu = 23 \end{cases} \quad (86)$$

and

$$[Z_1^{\mu\nu}]_S = \frac{1}{\gamma_p} \begin{cases} 0 & \mu\nu = 12 \\ -q \cos \theta_q & \mu\nu = 02 \\ \omega & \mu\nu = 23 \end{cases} \quad (87)$$

with no allowed N components. For the tensors of type 2 one has

$$h_p \gamma_p Z_2^{2\mu} = T^\mu Z_0,$$

with $\mu = 0, 1, \text{ or } 3$ and

$$Z_0 \equiv \epsilon^{2\alpha'\beta'\gamma'} S_{\alpha'}^p T_{\beta'} Q_{\gamma'} \quad (88)$$

yielding

$$h_p [Z_0]_L = -m_p q \sin \theta_q \quad (89)$$

$$h_p [Z_0]_S = -[p\omega + Eq \cos \theta_q] \quad (90)$$

$$[Z_0]_N = 0. \quad (91)$$

The polarized contraction in Eq. (85) is then given by

$$X^{pol} = -h_e h_p 4EG_M^p C^{pol}, \quad (92)$$

where

$$C^{pol} \equiv \frac{1}{8m_p^3} z_{\mu\nu} Z^{\mu\nu} \equiv G_M^p C_1^{pol} + F_2^p C_2^{pol} \quad (93)$$

$$= \frac{1}{4m_p^3} (z_{12} Z^{12} + z_{02} Z^{02} + z_{23} Z^{23}) \quad (94)$$

with $z_{\mu\nu}$ from Eq. (52) and $Z^{\mu\nu}$ from the developments given above, with the subscripts 1 and 2 referring to the two contributions in $Z^{\mu\nu}$. The extra factor of 2 in Eq. (94) comes from using the antisymmetry together with only one order of the indices $\mu\nu$. Again employing dimensionless variables one has

$$C_{1L}^{pol} = -\frac{1}{\gamma_p} [\tau^2 + \tilde{\epsilon} \kappa^2 \sin^2 \theta_q] \quad (95)$$

$$C_{1S}^{pol} = \kappa \sin \theta_q \left\{ (\lambda + \beta_p \kappa \cos \theta_q) \sqrt{\tilde{\epsilon}^2 - (m_e/m_p)^2} - (\beta_p \lambda + \kappa \cos \theta_q) \tilde{\epsilon} \right\} \quad (96)$$

$$C_{2L}^{pol} = \frac{1}{\gamma_p} \tilde{\epsilon} \kappa^2 \sin^2 \theta_q \quad (97)$$

$$C_{2S}^{pol} = \tilde{\epsilon} \kappa \sin \theta_q (\beta_p \lambda + \kappa \cos \theta_q), \quad (98)$$

where the result in Eq. (96) is obtained using the facts that

$$k = E \sqrt{\tilde{\epsilon}^2 - (m_e/m_p)^2} - p \tilde{\epsilon} \quad (99)$$

$$\epsilon = E \tilde{\epsilon} - p \sqrt{\tilde{\epsilon}^2 - (m_e/m_p)^2}. \quad (100)$$

It can be shown that C_{1L}^{pol} , C_{2L}^{pol} and C_{2S}^{pol} are all of order unity when $\gamma_p \rightarrow \infty$, whereas C_{1S}^{pol} goes as $1/\gamma_p$ in that limit. Furthermore, if one sets $F_1^p = 1$ and $F_2^p = 0$, then, through Eqs. (69), one has $G_E^p = G_M^p = 1$, and thus no terms of type 2 contribute (no terms involving C_{2L}^{pol} or C_{2S}^{pol}). This special case makes the proton current take on the same form as that of a point Dirac particle like the electron. Accordingly one sees that the only surviving contribution in the extreme relativistic limit for collisions of point Dirac particles is the one involving C_{1L}^{pol} , as expected. This also underlines the fact that the sideways contribution in the general case for ultra-relativistic protons arises because of the anomalous magnetic moment, *i.e.*, the parts of the current involving F_2 .

Finally, using the relationship for the Pauli form factor in terms of Sachs form factors (Eqs. (69)) and defining

$$C_M^{pol} \equiv \frac{1}{1+\tau} [(1+\tau)C_1^{pol} + C_2^{pol}] \quad (101)$$

$$C_E^{pol} \equiv \frac{1}{1+\tau} [-C_2^{pol}], \quad (102)$$

then one can write

$$C^{pol} = C_M^{pol} G_M^p + C_E^{pol} G_E^p. \quad (103)$$

From above we therefore have that

$$C_{ML}^{pol} = -\frac{1}{\gamma_p} \frac{\tau}{1+\tau} [\tau(1+\tau) + \tilde{\epsilon} \kappa^2 \sin^2 \theta_q] \quad (104)$$

$$C_{MS}^{pol} = \frac{1}{1+\tau} \kappa \sin \theta_q \left\{ (1+\tau)(\lambda + \beta_p \kappa \cos \theta_q) \times \sqrt{\tilde{\epsilon}^2 - (m_e/m_p)^2} - \tau (\beta_p \lambda + \kappa \cos \theta_q) \tilde{\epsilon} \right\} \quad (105)$$

$$C_{EL}^{pol} = -\frac{1}{\gamma_p} \frac{1}{1+\tau} \tilde{\epsilon} \kappa^2 \sin^2 \theta_q \quad (106)$$

$$C_{ES}^{pol} = -\frac{1}{1+\tau} \tilde{\epsilon} (\beta_p \lambda + \kappa \cos \theta_q) \kappa \sin \theta_q. \quad (107)$$

Next we will want to check these results by going to the lab. frame where $p = 0$, $E = m_p$, $\beta_p = 0$, $\gamma_p = 1$, $\tilde{\epsilon} = \epsilon/m_p$, $\sqrt{\tilde{\epsilon}^2 - (m_e/m_p)^2} = k/m_p$, $\lambda = \tau$ and $\kappa =$

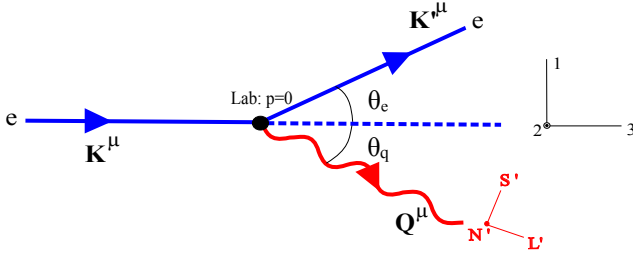


FIG. 4. (color online) Proton polarizations (L' , S' , N') in the lab. system where $p = 0$.

$\sqrt{\tau(1+\tau)}$. One has

$$\left[C_{ML}^{pol} \right]^{lab} = -\tau^2 \left(1 + \frac{\epsilon}{m_p} \sin^2 \theta_q \right) \quad (108)$$

$$\left[C_{MS}^{pol} \right]^{lab} = \tau \frac{1}{m_p} \left[\sqrt{\tau(1+\tau)} k - \tau \epsilon \cos \theta_q \right] \sin \theta_q \quad (109)$$

$$\left[C_{EL}^{pol} \right]^{lab} = -\tau \frac{\epsilon}{m_p} \sin^2 \theta_q \quad (110)$$

$$\left[C_{ES}^{pol} \right]^{lab} = -\tau \frac{\epsilon}{m_p} \sin \theta_q \cos \theta_q. \quad (111)$$

In the lab. system the polarizations of the proton are usually specified with respect to the (L' , S' , N') coordinate system as shown in Fig. 4. Rotating to this system one has

$$\left[C_{XL'}^{pol} \right]^{lab} = -\cos \theta_q \left[C_{XL}^{pol} \right]^{lab} + \sin \theta_q \left[C_{XS}^{pol} \right]^{lab} \quad (112)$$

$$\left[C_{XS'}^{pol} \right]^{lab} = -\sin \theta_q \left[C_{XL}^{pol} \right]^{lab} - \cos \theta_q \left[C_{XS}^{pol} \right]^{lab} \quad (113)$$

with $X = M$ or E . After some algebra one finds that

$$\left[C_{ML'}^{pol} \right]^{lab} = \tau \left[\tau \cos \theta_q + \sqrt{\tau(1+\tau)} \frac{k}{m_p} \sin^2 \theta_q \right] \quad (114)$$

$$\left[C_{MS'}^{pol} \right]^{lab} = 0 \quad (115)$$

$$\left[C_{EL'}^{pol} \right]^{lab} = 0 \quad (116)$$

$$\left[C_{ES'}^{pol} \right]^{lab} = \frac{\epsilon}{m_p} \tau \sin \theta_q, \quad (117)$$

where the zeros in Eqs. (115) and (116) are expected from the familiar lab. frame analysis.

V. THE CROSS SECTION AND POLARIZATION ASYMMETRY

Finally in these developments of the formalism, we now want to obtain the cross section and polarization asymmetry in the collider frame, together with their lab. frame

and extreme relativistic limits. We begin with the unpolarized cross section in the general collider frame. First, the flux factor to be used in applying the Feynman rules must now be generalized (see [6], Eqs. (7.41) and (B.1): where in the lab. frame one has the multiplicative factor $1/\beta_e \gamma_e$ one now has the replacement

$$\frac{1}{\beta_e \gamma_e} \rightarrow \frac{1}{\gamma_e \gamma_p (\beta_e + \beta_p)}, \quad (118)$$

where both factors of β are to be taken positive. Clearly the lab. frame result emerges when $\beta_p \rightarrow 0$ and $\gamma_p \rightarrow 1$. The recoil factor can be shown to generalize to

$$F_{rec} = 1 + \frac{\epsilon k' - \epsilon' (k - p) \cos \theta_e}{E k'} \quad (119)$$

and using V_0 given in Eq. (76) one has

$$\left[\frac{d\sigma}{d\Omega_e} \right]_{ep}^{unpol, collider} = \sigma_M^{collider} (F_{rec})^{-1} F^2(\tau, \theta_e) \quad (120)$$

with the square of the form factor from Eq. (81) and the generalized Mott cross section given by

$$\sigma_M^{collider} = \left(\frac{\alpha}{Q^2} \right)^2 \frac{k'}{k} V_0 \frac{\beta_e}{\beta_e + \beta_p} \frac{1}{\gamma_p^2}. \quad (121)$$

These results can be checked by going to the lab. frame and shown to agree with the familiar answers.

Various limiting cases may be straightforwardly obtained. First, in the ERL_e one has

$$F_{rec}^{ERL_e} = 1 + \beta_p \cos \theta_e \quad (122)$$

$$\tilde{\epsilon}^{ERL_e} = \frac{k}{m_p} \gamma_p (1 + \beta_p) \quad (123)$$

$$\sigma_M^{collider, ERL_e} = \left(\frac{\alpha}{Q^2} \right)^2 \frac{k'}{k} V_0^{ERL_e} \frac{1}{1 + \beta_p} \frac{1}{\gamma_p^2} \quad (124)$$

where $V_0^{ERL_e}$ may be obtained using Eq. (76) and therefore $\sigma_M^{collider, ERL_e}$ using Eq. (121).

With both beams polarized the cross section has two terms, one (Σ) containing no dependence on the polarizations and one (Δ) containing only terms where both beams are polarized [7], the latter being proportional to the product $h_e h_p$:

$$\left[\frac{d\sigma}{d\Omega} \right]_{ep}^{pol, collider} \equiv \sigma^{h_e, h_p} = \Sigma + h_e h_p \Delta. \quad (125)$$

By flipping the spins one can form the polarization asymmetry:

$$[A]_{ep}^{pol, collider} \equiv \frac{\sigma^{+,+} - \sigma^{-,+}}{\sigma^{+,+} + \sigma^{-,+}} = \frac{\sigma^{+,+} - \sigma^{+,-}}{\sigma^{+,+} + \sigma^{+,-}} = \frac{\Delta}{\Sigma}. \quad (126)$$

Using the developments above we immediately have that

$$[A]_{ep}^{pol, collider} = \frac{h_e h_p X^{pol}}{X^{unpol}}, \quad (127)$$

where X^{unpol} is given in Eq. (79) and X^{pol} is defined in Eq. (85). Substituting for these and expressing C^{pol} in terms of G_M^p and G_E^p using Eq. (103) we find that

$$[A]_{ep}^{pol,collider} = -\frac{\mathcal{N}}{F^2(\tau, \theta_e)}, \quad (128)$$

where the numerator is given by

$$\begin{aligned} \mathcal{N} &\equiv \frac{2}{\tau} \gamma_p \tan^2 \theta'_e / 2 \left[G_M^p \left(C_M^{pol} G_M^p + C_E^{pol} G_E^p \right) \right] \\ &\equiv \mathcal{N}_M (G_M^p)^2 + \mathcal{N}_E G_E^p G_M^p \end{aligned} \quad (129)$$

and where $C_{M,E}^{pol}$ are given in Eqs. (104-107) for the two types of proton polarization, L and S . Again, for reference, the denominator in Eq. (128) is given in Eq. (81) and $\tan^2 \theta'_e / 2$ is given in Eq. (78).

As a first check, let us go to the lab. frame and consider the L' and S' polarizations discussed above. We have from Eq. (114) that the L' part of the numerator in Eq. (129) in the lab. frame where $\theta'_e \rightarrow \tilde{\theta}_e$ is given by

$$\begin{aligned} &-\frac{2}{\tau} \tan^2 \tilde{\theta}_e / 2 \left[C_{ML'}^{pol} \right]^{lab} (G_M^p)^2 \\ &= -2 \tan^2 \tilde{\theta}_e / 2 \\ &\quad \times \left[\tau \cos \theta_q + \sqrt{\tau(1+\tau)} \frac{k}{m_p} \sin^2 \theta_q \right] (G_M^p)^2 \\ &\equiv V_{T'} W_{L'}^{T'}, \end{aligned} \quad (131)$$

using a notation where

$$W_{L'}^{T'} = -2\tau (G_M^p)^2. \quad (132)$$

This implies that

$$\begin{aligned} V_{T'} &= \frac{1}{\tau} \tan^2 \tilde{\theta}_e / 2 \\ &\quad \times \left[\tau \cos \theta_q + \sqrt{\tau(1+\tau)} \frac{k}{m_p} \sin^2 \theta_q \right] \\ &= \frac{1}{\beta} \tan^2 \tilde{\theta}_e / 2 \\ &\quad \times \left(\frac{\epsilon + \epsilon'}{q} \right) \left[1 - \frac{2m_e^2 q^2}{\epsilon(\epsilon + \epsilon')(-Q^2)} \right], \end{aligned} \quad (133)$$

which agrees with the standard notation (*e.g.*, see [4]). The S' part of the numerator in Eq. (128) in the lab. frame is found similarly:

$$\begin{aligned} &-\frac{2}{\tau} \tan^2 \tilde{\theta}_e / 2 \left[C_{ES'}^{pol} \right]^{lab} G_E^p G_M^p = 2 \tan^2 \tilde{\theta}_e / 2 \\ &\quad \times \left(\frac{\epsilon}{m_p} \right) \sin \theta_q G_E^p G_M^p \end{aligned} \quad (134)$$

$$\equiv V_{T'} W_{S'}^{T'}, \quad (135)$$

again using the notation where

$$W_{S'}^{T'} = 2\sqrt{2\tau(1+\tau)} G_E^p G_M^p \quad (136)$$

yielding

$$V_{TL'} = -\frac{1}{v_0} \sqrt{2} \frac{\tau}{\kappa^2} \epsilon k' \sin \theta_e, \quad (137)$$

which agrees with the standard notation (*e.g.*, see [4]).

Finally, for the crossed beams situation one must extend the discussion of the leptonic and hadronic tensors in Sect. III. In this case it is more convenient to work in the (1, 2, 3) system. The leptonic tensor will be as before; however, the hadronic tensor will now be assumed to have L and S polarizations with respect to the rotated frame. That is, we will assume that L- or S-polarizations occur when the proton's polarization lies along the directions

$$\mathbf{u}_{L,crossed} = -\mathbf{u}_{z'} = \sin \chi \mathbf{u}_1 - \cos \chi \mathbf{u}_3 \quad (138)$$

$$\mathbf{u}_{S,crossed} = -\mathbf{u}_{x'} = -\cos \chi \mathbf{u}_1 - \sin \chi \mathbf{u}_3. \quad (139)$$

Accordingly the asymmetries in the crossed beams situation are simply linear combinations of the collinear ones that we derived in Sect. V:

$$\begin{aligned} [A]_{ep}^{pol,collider} \Big|_{L,crossed} &= -\sin \chi [A]_{ep}^{pol,collider} \Big|_{S,collinear} \\ &\quad + \cos \chi [A]_{ep}^{pol,collider} \Big|_{L,collinear} \end{aligned} \quad (140)$$

$$\begin{aligned} [A]_{ep}^{pol,collider} \Big|_{S,crossed} &= \cos \chi [A]_{ep}^{pol,collider} \Big|_{S,collinear} \\ &\quad + \sin \chi [A]_{ep}^{pol,collider} \Big|_{L,collinear} \end{aligned} \quad (141)$$

It is straightforward to verify that all of the collinear results obtained above are recovered when the crossing angle χ is set to zero.

VI. PARITY-VIOLATING ELASTIC ELECTRON SCATTERING

While our main focus in the present work is placed on the double-polarization reaction $\vec{p}(\vec{e}, e)p$ where parity-conserving (PC) asymmetries occur, it is interesting also to consider in context parity-violating (PV) single-polarization $p(\vec{e}, e)p$ scattering. The general structure of PV elastic electron scattering from the proton is illustrated in Fig. 5. Two diagrams are relevant: the usual photon exchange diagram which is parity conserving and a Z^0 exchange diagram which has both polar vector (V) and axial vector (A) contributions. To obtain the total cross section one must take the sum of these two diagrams and compute the square of the absolute value of that sum, leading to terms from the square of the photon exchange diagram (VV) which are parity conserving, terms from the interferences between the two diagrams which include VA pieces that are parity violating (PV) and pieces from the square of the Z^0 exchange diagram which are very small and so neglected. Upon considering longitudinally polarized electron scattering elastic from *unpolarized* protons, the electron spin asymmetry can only occur from parity violations and thus the VA interferences are the leading-order PV contributions. The

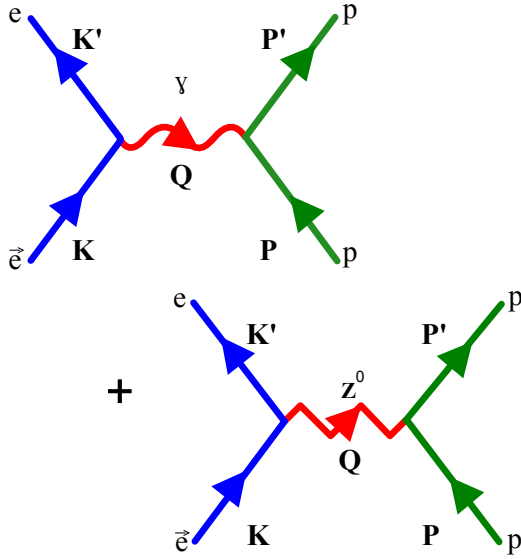


FIG. 5. (color online) Parity-violating electron-proton elastic scattering.

details of the developments of the PV formalism are given in several references [8, 9] and here we only summarize the differences that occur when working in the collider frame. We begin with a brief discussion of the leptonic and hadronic tensors involved.

In these developments for simplicity we consider only the extreme relativistic limit for the electrons. In Sect. III the leptonic tensor for the unpolarized situation was given (see Eq. (46)):

$$\chi_{\mu\nu}^{(s)} \equiv \frac{1}{2}Q^2 \left(g_{\mu\nu} - \frac{Q_\mu Q_\nu}{Q^2} \right) + 2R_\mu R_\nu \quad (144)$$

which is symmetric under interchange of μ and ν . Now, since the weak interaction has both vector and axial vector contributions, a second tensor must be considered:

$$\chi_{\mu\nu}^{(a)} \equiv i\epsilon_{\mu\nu\alpha\beta} Q^\alpha R^\beta, \quad (145)$$

which is antisymmetric under interchange of μ and ν , and the full lepton tensor for the helicity-difference matrix elements may be written

$$\chi_{\mu\nu}^{\text{PV, hel. diff.}} = a_A \chi_{\mu\nu}^{(s)} + a_V \chi_{\mu\nu}^{(a)}, \quad (146)$$

where the Standard Model electroweak couplings are

$$a_V = -(1 - 4 \sin^2 \theta_W) \simeq -0.092 \quad (147)$$

$$a_A = -1 \quad (148)$$

using for the weak mixing angle the value $\sin^2 \theta_W \simeq 0.227$.

The hadronic (proton) tensor is similar: the symmetric tensor is the analog of the unpolarized tensor given in Eq. (60)

$$\widetilde{W}_{(s)}^{\mu\nu} = -\widetilde{W}_1 \left(g^{\mu\nu} - \frac{Q^\mu Q^\nu}{Q^2} \right) + \frac{1}{m_p^2} \widetilde{W}_2 T^\mu T^\nu \quad (149)$$

which has the same form as the unpolarized proton tensor, but with different structure functions $\widetilde{W}_{1,2}$ to be discussed below; these are differentiated by the tildes in Eq. (149). Likewise the antisymmetric proton tensor that is the analog of that in Eq. (145) is

$$\widetilde{W}_{(a)}^{\mu\nu} = \frac{i}{m_p^2} \widetilde{W}_3 \epsilon^{\mu\nu\alpha'\beta'} Q_{\alpha'} T_{\beta'} \quad (150)$$

with an additional structure function \widetilde{W}_3 .

The structure functions (functions only of τ) occurring above in Eq. (149) are the analogs of the familiar $W_{1,2}$ in PC elastic e-p scattering given above (see Sect. III) except that the PV analogs involve interferences between the γ and Z^0 diagrams and so contain products of EM form factors and their weak neutral current counterparts (indicated with tildes; see [8]):

$$\widetilde{W}_1 = \tau G_M^p \widetilde{G}_M^p \quad (151)$$

$$\widetilde{W}_2 = \frac{1}{1 + \tau} \left[G_E^p \widetilde{G}_E^p + \tau G_M^p \widetilde{G}_M^p \right]. \quad (152)$$

These are all of polar vector type and go with the leptonic axial vector term (*i.e.*, proportional to a_A) to make the VA interference. The antisymmetric case has a leptonic part that is a polar vector, but an interference of one polar and one axial vector contribution for the proton to make the VA interference (see [8]):

$$\widetilde{W}_3 = -\frac{1}{2} G_M^p \widetilde{G}_A^p. \quad (153)$$

Finally, the weak neutral current form factors in the Standard Model are the following

$$\widetilde{G}_E^p = \frac{1}{2} \left[(1 - 4 \sin^2 \theta_W) G_E^p - G_E^n - G_E^{(s)} \right] \quad (154)$$

$$\widetilde{G}_M^p = \frac{1}{2} \left[(1 - 4 \sin^2 \theta_W) G_M^p - G_M^n - G_M^{(s)} \right] \quad (155)$$

$$\widetilde{G}_A^p = \frac{1}{2} \left[G_A^{(1)} - G_A^{(s)} \right], \quad (156)$$

where now the neutron's electromagnetic form factors $G_{E,M}^n$ enter, there are potential strangeness form factors $G_{E,M,A}^{(s)}$ and the axial vector, isovector form factor $G_A^{(1)}$ (that, for instance, enters in $n \rightarrow p$ β -decay) occurs in Eq. (156).

When contracting these leptonic and hadronic tensors, of course only the symmetric or antisymmetric contributions contract with one another and no cross terms (symmetric times antisymmetric) can occur. The results are the following: for the contraction of the symmetric tensors we have

$$\chi_{\mu\nu}^{(s)} \widetilde{W}_{(s)}^{\mu\nu} = -Q^2 \widetilde{W}_1 + 2m_p^2 [\tilde{\epsilon}^2 - 2\tau\tilde{\epsilon} - \tau] \widetilde{W}_2 \quad (157)$$

$$= \frac{1}{2} V_0 \left(\widetilde{W}_2 + 2\widetilde{W}_1 \tan^2 \theta'_e/2 \right), \quad (158)$$

where $\tilde{\epsilon}$ is defined via Eq. (74) and the last equality comes from using Eq. (76); these developments completely parallel the unpolarized contraction discussed in Sect. IV.

Note that the result here again involves the definition of an effective angle, *i.e.*, Eq. (78). For the contraction of the antisymmetric tensors the result is

$$\chi_{\mu\nu}^{(a)} \widetilde{W}_{(a)}^{\mu\nu} = -8m_p^2 \tau (\tilde{\epsilon} - \tau) \widetilde{W}_3 \quad (159)$$

$$= \frac{1}{2} V_0 \frac{\tau (\tilde{\epsilon} - \tau)}{\tilde{\epsilon}^2 - 2\tau\tilde{\epsilon} - \tau} \left(-2\widetilde{W}_3 \right). \quad (160)$$

These results are for a general frame and thus may be used directly in the collider frame.

Using the explicit results for the ERL_e the PV asymmetry may be written

$$\mathcal{A}_{PV} = \mathcal{A}_{PV}^0 \frac{\mathcal{N}_{PV}}{\mathcal{D}_{PV}}, \quad (161)$$

where

$$\mathcal{A}_{PV}^0 = \frac{G|Q^2|}{2\pi\alpha\sqrt{2}} = \frac{\sqrt{2}G\tau}{\pi\alpha} \simeq 6.33423 \times 10^{-4} \tau \quad (162)$$

with G the Fermi weak coupling constant. The denominator in Eq. (161) comes from the helicity sum cross section, namely, the PC elastic electron scattering cross section discussed above. Omitting factors that are common to the numerator it may be written

$$\mathcal{D}_{PV} = \mathcal{E}' (G_E^p)^2 + \tau (G_M^p)^2, \quad (163)$$

namely, proportional to the familiar result involving the EM form factors (see Sect. IV). The numerator arises from the PV helicity difference cross section using the contractions developed above:

$$\begin{aligned} \mathcal{N}_{PV} = a_A \left\{ \mathcal{E}' G_E^p \tilde{G}_E^p + \tau G_M^p \tilde{G}_M^p \right\} \\ + a_V \left\{ \sqrt{1 - \mathcal{E}'^2} \sqrt{\tau(1 + \tau)} G_M^p \tilde{G}_A^p \right\}. \end{aligned} \quad (164)$$

Finally, the expressions above may be checked (see [8]) by going to the lab. frame, where for the ERL_e $\mathcal{E}' \rightarrow \mathcal{E}$.

VII. TYPICAL RESULTS FOR E-P SCATTERING IN COLLIDER KINEMATICS

In presenting results in this section we have made two choices for specific kinematics, a high-energy choice that may be typical of a future EIC facility and a somewhat lower-energy one where it may be possible to make measurements of the proton EM form factors at a level of precision that is interesting (see below). The two choices are listed in Table I along with rest-frame variables corresponding to typical collider-frame scattering angles, $\theta_e = 1^\circ$ and 5° — see the discussions below.

For use in assessing the feasibility of performing asymmetry measurements one frequently employs the so-called Figure-of-Merit (FOM):

$$\mathcal{F} \equiv \left[\frac{d\sigma}{d\Omega_e} \right]_{ep}^{unpol, collider} \left([A]_{ep}^{pol, collider} \right)^2. \quad (165)$$

	Kinematics I	Kinematics II
k (GeV/c)	10	2
p (GeV/c)	250	50
k_{rest} (GeV/c)	5329	213.2
θ_e^{rest} (deg) at $\theta_e = 1^\circ$	0.00188	0.00938
$\tan(\theta_e^{rest}/2)$ at $\theta_e = 1^\circ$	1.638×10^{-5}	8.187×10^{-5}
$1 - \mathcal{E}$ at $\theta_e = 1^\circ$	5.410×10^{-10}	1.341×10^{-8}
θ_e^{rest} (deg) at $\theta_e = 5^\circ$	0.00939	0.0469
$\tan(\theta_e^{rest}/2)$ at $\theta_e = 5^\circ$	8.193×10^{-5}	4.096×10^{-4}
$1 - \mathcal{E}$ at $\theta_e = 5^\circ$	1.633×10^{-8}	3.385×10^{-7}

TABLE I. Selected kinematics and rest-frame variables.

Also, to incorporate the fact that the solid angle goes as $\sin \theta_e$, it is also appropriate to consider the product $\mathcal{F} \sin \theta_e$. Given luminosity L , electron polarization p_e , proton polarization p_p , run time T and an averaged FOM times solid angle

$$\mathcal{F}_{avg} \Delta\Omega_e \equiv \int_{\theta_0}^{\theta_e} \mathcal{F} \sin \theta'_e d \sin \theta'_e, \quad (166)$$

where θ_0 is whatever one wishes to choose for the lower limit of integration over scattering angle (written in the integrand above as θ'_e to avoid confusion with θ_e which has been used above and has a different meaning) and where the full 2π integration in azimuthal angle has been assumed, the fractional uncertainty in the L or S asymmetry is given by

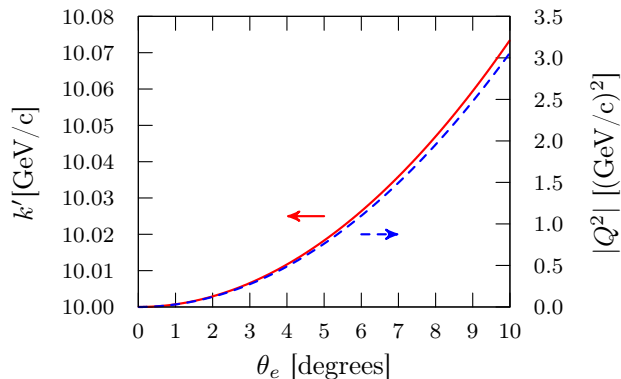
$$f = \left\{ p_e p_p \sqrt{LT \mathcal{F}_{avg} \Delta\Omega_e} \right\}^{-1}. \quad (167)$$

For the results to follow we have assumed the conditions listed in Table II. For simplicity the lower limit chosen for the averaging of the FOM has been fixed to $\theta_0 = 0^\circ$ for the results shown in the figures; the time assumed is relatively short. In any practical situation these two parameters will need to be adjusted to find the optimal choices. The present study is not intended to be more than a preliminary exploration of typical results and so no attempt has been made to optimize the choices here. On the other hand, a general program, Brasil2011, has been developed to study $\vec{e}\text{-}\vec{p}$ scattering in collider kinematics. The code, together with a description and sample input/output are available [2]. All of the parameters above can be chosen by the user. In addition, the program provides the option of choosing between two models for computing the nucleon form factors, namely, a simple model which gives a reasonable starting point for e-p studies and the vector meson dominance plus pQCD GKex model which yields good agreement with most of the World form factor data (see [10] and references cited therein for details). Alternatively, it is straightforward for any user to provide other form factor representations. In the following we show selected results using this code with the GKex form factors.

In Fig. 6 the scattered electron's 3-momentum k' (left axis) and $|Q^2|$ (right axis) are shown as functions of the electron scattering angle for kinematics I; the range of

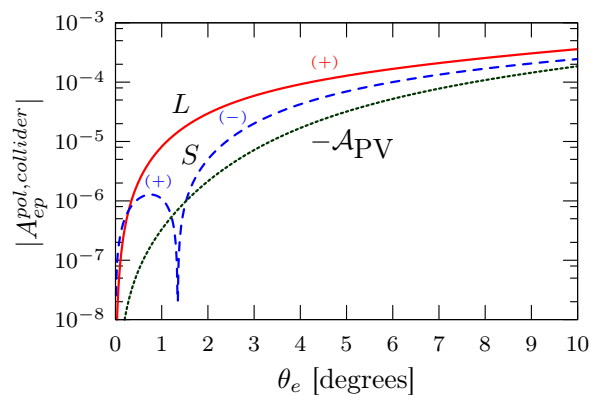
$$\begin{aligned}
L &= 10^{34} \text{ cm}^{-2} \text{ s}^{-1} \\
p_e &= 90\% \\
p_p &= 70\% \\
T &= 1000 \text{ hr} \\
\theta_0 &= 0^\circ
\end{aligned}$$

TABLE II. Assumed experimental conditions.

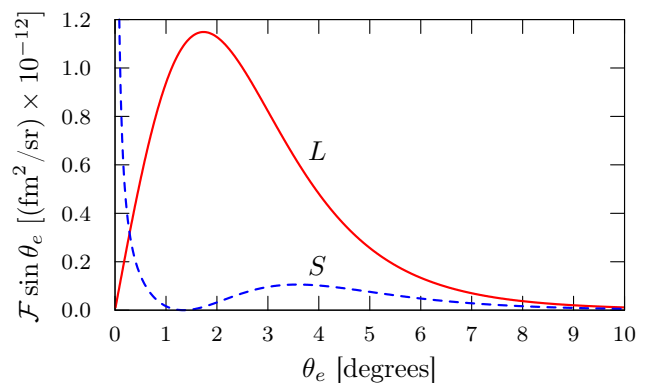
FIG. 6. (color online) Kinematics I: scattered electron 3-momentum k' and 4-momentum transfer squared $|Q^2|$ versus collider-frame electron scattering angle θ_e .

angles chosen here is dictated by where the FOM is significant, as seen later in Fig. 8. Clearly k' does not vary significantly over the chosen range of angles, less than 75 MeV/c out of about 10 GeV/c. For the same range of angles the scattered proton 3-momentum goes from 250 GeV/c at $\theta_e = 0^\circ$ down by only about 75 MeV/c at 10° while scattering through an angular range of $\theta_p = 0^\circ$ at $\theta_e = 0^\circ$ to $\theta_p = 0.4^\circ$ at $\theta_e = 10^\circ$. It is clear from our initial exploratory studies that energy resolution alone is rather unlikely to be enough to separate elastic events from inelastic ones (the code Brasil2011 contains some kinematic developments where the final hadronic state can be taken to have invariant mass $W \neq m_p$) and some final-state particle identification will likely be needed to isolate elastic scattering in practical situations.

In Fig. 7 the asymmetries are shown for the same range of electron scattering angles used above. The $\vec{\epsilon} \cdot \vec{p}$ L polarization is larger in magnitude than for the S case, although the two are comparable. The latter changes sign at roughly $\theta_e = 1.3^\circ$. In the region where the FOM peaks (roughly $\theta_e \sim 2^\circ$; see Fig. 8) the L asymmetry is a few times 10^{-5} . One might be surprised that this is so low. The reason is clear upon examining the rest-frame variables in Table I: $\tan(\theta_e^{rest}/2)$ goes from 1.6×10^{-5} at $\theta_e = 1^\circ$ to 8.2×10^{-5} at $\theta_e = 5^\circ$. Since the asymmetries are proportional either to the generalized ‘‘Rosenbluth’’ factor V_T for L polarization or to V_{TL} for S polarization (see Sect. V) and these both have an overall factor $\tan(\theta_e^{rest}/2)$ in the rest frame [4], the kinematical factors are small. In other words, the scattering in the equivalent rest frame occurs at such small angles that the double-polarization asymmetries are suppressed. For compari-

FIG. 7. (color online) Kinematics I: double-polarization asymmetries $[A]_{ep}^{pol,collider}$ for L and S proton polarizations versus electron scattering angle θ_e . Also shown is the parity-violating e-p elastic asymmetry \mathcal{A}_{PV} for the same kinematics.

son the parity-violating asymmetry \mathcal{A}_{PV} is also shown in Fig. 7. In this case, even though the weak interaction is involved, some of the contributions occurring in the ratio forming the asymmetry (see Sect. VI) are not suppressed by similar factors. In the same notation used above the Rosenbluth factors V_L and V_T occur for the VV hadronic contributions (those involving $G_{E,M}^p, \tilde{G}_{E,M}^p$ in Eq. (164)) and these do not contain overall factors of $\tan(\theta_e^{rest}/2)$. On the other hand, the VA interference in Eq. (164) (involving G_M^p, \tilde{G}_A^p) has a factor $\sqrt{1 - \mathcal{E}^2}$ and so is strongly suppressed (see Table I).

FIG. 8. (color online) Kinematics I: $\mathcal{F} \sin \theta_e$ versus electron scattering angle θ_e .

Another observation from Table I is that the smallness of $1 - \mathcal{E}$, going from 5.4×10^{-10} at $\theta_e = 1^\circ$ to 1.6×10^{-8} at $\theta_e = 5^\circ$, implies something very different about any potential 2γ corrections to the dominantly 1γ diagram. Namely, from treatments of the former (*e.g.*, see [11]) one expects the 2γ contributions to vanish when $\mathcal{E} \rightarrow 1$, which is surely the case for the rest-frame-equivalent conditions studied here.

Figure 9 shows the fractional uncertainty obtained using Eq. (167) and implies that in a time $T = 1000$ hr one

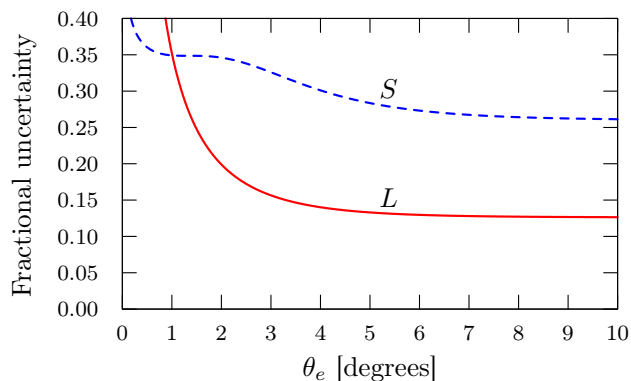


FIG. 9. (color online) Kinematics I: fractional uncertainty f (see Eq. (167)) for polarizations L and S versus electron scattering angle θ_e .

could achieve roughly a 15–20% determination of the L polarization asymmetry. Since the fractional uncertainty goes as $1/\sqrt{T}$, clearly with longer run times even higher precision can be obtained.

For kinematics II the results are shown in Figs. 10, 11, 12 and 13. Now the angular range is larger (θ_e up to 20°), again as dictated by the significance of the FOM (see Fig. 12 below). The scattered proton's 3-momentum k' in this case varies from 50 GeV/c at $\theta_e = 0^\circ$ to 15 MeV/c less than this at 10° , while the proton's scattering angle θ_p goes from 0° up to 0.4° over the same range. The asymmetries are shown in Fig. 11: these are significantly larger than was the case for kinematics I and now lie typically two or more orders of magnitude above the PV asymmetry. Figure 12 shows the FOM and indicates that for the L polarization case a peak occurs for θ_e between 8° and 9° . This yields the fractional uncertainty displayed in Fig. 13, clearly showing that a 1–2% determination of the asymmetries may be possible, given the assumed luminosity, polarizations and run time.

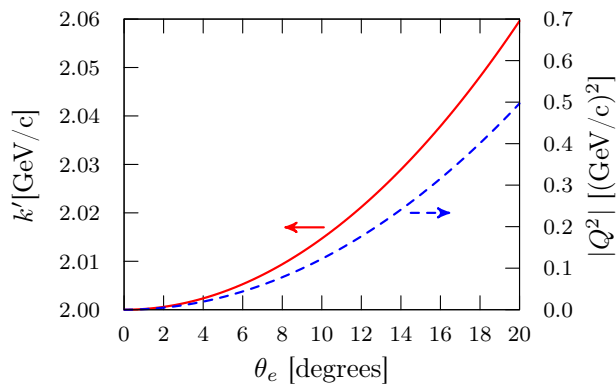


FIG. 10. (color online) As for Fig. 6, but now for kinematics II.

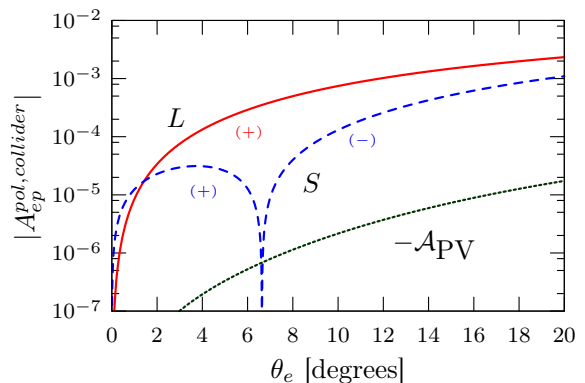


FIG. 11. (color online) As for Fig. 7, but now for kinematics II.

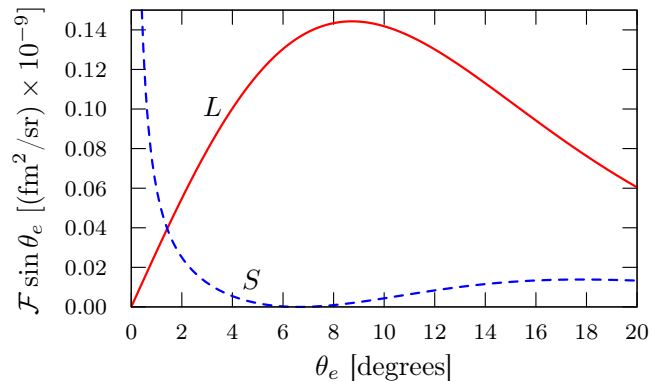


FIG. 12. (color online) As for Fig. 8, but now for kinematics II.

VIII. CONCLUSIONS

In this study elastic $\vec{e}\vec{p}$ cross sections and asymmetries have been considered in collider kinematics. The formalism has been developed directly using the electron and proton tensors and working in a general frame — since the resulting expressions are covariant it is easy

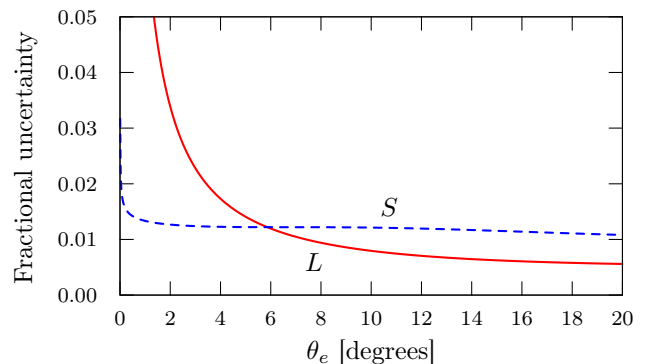


FIG. 13. (color online) As for Fig. 9, but now for kinematics II.

to evaluate the results in any chosen frame, including the system where the proton is at rest and where the asymmetries and cross sections are well known, thereby providing a sensitive check on the formalism. In context, parity-violating elastic $\bar{e}p$ scattering has also been explored in collider kinematics to be able to compare and contrast the resulting asymmetry with the double-polarization (parity-conserving) results.

Several observations and conclusions can be made from these studies:

- The double-polarization asymmetries are relatively small, since the effective rest-frame electron scattering angle is very small for typical collider kinematics and since both the L and S asymmetries in the rest frame have an overall factor of $\tan(\theta_e^{rest}/2)$. In contrast, the PV asymmetry has contributions that do not contain this factor and therefore survive when the electron scattering angle becomes very small. Indeed, for some kinematical situations the PV asymmetry is only about one order of magnitude smaller than the PC asymmetries.
- The L and S asymmetries, while small, are still sufficiently large that it may prove possible to make relatively high-precision measurements of them with a future EIC facility as it is presently envisioned. If, with such a facility, it proves possible to use beams that have a large dynamical range, including lower energies and beams that are more symmetrical in energy (the EIC designs being considered are typically asymmetric with the proton beam being much higher in energy than the electron beam), then very likely quite high-quality determinations of the double-polarization asymmetries can be made.
- Given that the double-polarization asymmetries can be measured with sufficient precision two paths may be followed: (1) the proton EM form factors themselves may be studied; and given that we know these form factors reasonably well from fixed-target experiments, (2) the asymmetries may be used to determine the product of the electron and proton polarizations when the focus is on other e-p reactions, including studies of DIS.
- With respect to point (1) above, the collider kinematics are very unusual in that the effective rest-frame kinematics typically occur at very large energies and very small angles. This means that the virtual photon longitudinal polarization \mathcal{E} is extremely close to unity where it is predicted that 2γ corrections to the dominantly 1γ diagram go to zero.
- Specifics of how the proton EM form factors enter the asymmetries are interesting: if the anomalous magnetic or Pauli form factor F_2^p were zero, as is

the case for a point Dirac particle, then the L/S structure of the asymmetries would be quite different. The fact that $F_2^p \neq 0$ leads to clear signatures in the double-polarization asymmetries.

- Finally, while this work is a theoretical study and has been focused on the formalism plus presentations of a few typical results, some initial exploration has been made of the issues that will probably confront any practical experiment. In particular, it is very unlikely for high-energy collider kinematics that energy resolution alone will be capable of isolating elastic e-p scattering from inelastic scattering. Instead one will have to detect both the scattered electron and specify the final hadronic state including the elastic events where only the scattered proton occurs. This is not the point of the present study, although a computer code has been written and is available [2] for others involved in design studies for a future EIC facility.

APPENDIX

The conventions of Bjorken and Drell [6] are used throughout together with the follow notation: 4-vectors are written with capital letters

$$A^\mu = (A^0, A^1, A^2, A^3) = (A^0, \mathbf{a}) \quad (168)$$

$$A_\mu = (A^0, -A^1, -A^2, -A^3) = (A^0, -\mathbf{a}), \quad (169)$$

where 3-vectors are written with bold lowercase letters and their magnitudes with normal lowercase letters, $a = |\mathbf{a}|$. The scalar product of two 4-vectors A and B is given by

$$A \cdot B = A^\mu B_\mu = A^0 B^0 - \mathbf{a} \cdot \mathbf{b}, \quad (170)$$

where the summation convention is employed, namely repeated Greek indices are summed ($\mu = 0, 1, 2, 3$). Thus one has for the scalar product of a 4-vector with itself

$$A^2 = (A^0)^2 - a^2. \quad (171)$$

Throughout we use $\hbar = c = 1$.

ACKNOWLEDGMENTS

This work was supported in part by NSF Award 0754425 through the Hampton University UnIPhy-REU program and the MSRP program at MIT (CS) and in part by the U.S. Department of Energy under cooperative agreement DE-FC02-94ER40818 (TWD). The authors also wish to thank R. Milner and J. Bernauer of MIT for helpful discussions during the course of this study.

-
- [1] R. V. A. Deshpande, R. Milner and W. Vogelsang, *Ann. Rev. Nucl. Part. Sci.*, **55**, 165 (2005), arXiv:hep-ph/0506148 [hep-ph].
- [2] The C++ computer code Brasil2011 that yields all of the kinematic variables, cross sections, asymmetries and figures-of-merit may be obtained by contacting c.sofiatti@gmail.com.
- [3] NB: in the conventions employed in this and other work upon which these studies are based the 4-vector conventions outlined in the Appendix are adopted and consequently Q^2 is negative when spacelike.
- [4] T. Donnelly and A. Raskin, *Ann. Phys. (NY)*, **169**, 247 (1986).
- [5] Note that the angle θ'_e defined via Eq. (78) is not the true scattering angle, but is an effective angle that makes the expressions to follow relatively compact. When one goes to the proton rest system and invokes the electron extreme relativistic limit this primed angle reverts to the true scattering angle θ_e .
- [6] J. Bjorken and S. Drell, *Relativistic quantum mechanics* (McGraw-Hill, 1964).
- [7] Here we consider only parity-conserving $e-p$ scattering; for the parity-violating situation where only the electron beam is assumed to be polarized, see Sect. VI.
- [8] T. Donnelly, J. Dubach, and I. Sick, *Phys. Rev. C*, **37**, 2320 (1988).
- [9] M. Musolf, T. Donnelly, J. Dubach, S. Pollock, S. Kowalski, *et al.*, *Phys. Rept.*, **239**, 1 (1994).
- [10] C. Crawford, T. Akdogan, R. Alarcon, W. Bertozzi, E. Booth, *et al.*, *Phys. Rev. C*, **82**, 045211 (2010), arXiv:1003.0903 [nucl-th].
- [11] J. Guttmann, N. Kivel, and M. Vanderhaeghen, (2011), arXiv:1101.5967 [hep-ph].